JOURNAL OF AEROSPACE COMPUTING, INFORMATION, AND COMMUNICATION
Vol. 3, November 2006

Intelligent Star Pattern Recognition for Attitude Determination: the "Lost in Space" Problem

Lalitha Paladugu, Ebenezer Seisie-Amoasi, Brian G. Williams,* and Marco P. Schoen
Idaho State University, Pocatello, ID 83209, USA

This paper presents a novel approach to the attitude determination problem of space vehicles. The proposed algorithm utilizes a modified Genetic Algorithm (GA) to solve the "lost in space" star pattern recognition problem associated with star tracker attitude determination systems. Characteristics of the stars that are visible within the Field of View (FOV) – reflected on an image taken by the onboard star tracker – are formulated using simple geometric descriptions. The proposed GA minimizes the discrepancy between the characteristics of the stars inside the actual FOV and a candidate FOV selected from the on board stored star map. The global minimum of the discrepancy represents the inertial coordinates of the FOV bore-sight. The concept of a Spiral Genetic Algorithms (SGA) is proposed where the search area decreases for consecutive GA, with consequently tighter constraints, making it converge to the desired location. Also the algorithm presented has the capability of determining the rotational angle between the spacecraft's coordinate system and that of a real star map. Simulation results indicate competitive results to current star trackers in terms of accuracy.

I. Introduction

ATTITUDE, as applied to a spacecraft, expresses the rotational motion about its center of mass. Often it is desired to know the attitude of a spacecraft, or know the direction in which the spacecraft is pointed. Almost all spacecraft have attitude requirements for systems such as antenna or cameras. Controlling or changing the attitude can be accomplished with thrusters, momentum wheels, torque rods, to name a few, and is not discussed in this paper. Attitude measurement systems include sun sensors, earth horizon sensors, magnetometers, and star trackers, to name a few. Star trackers, the attitude determination system investigated in this paper, have the advantage of not requiring a solar system body, such as the sun or the earth, but rely on the known positions of cataloged celestial objects. Liebe[1] characterizes the operation of a star tracker as the matching process between an image taken from a known reference frame and some on board stored reference. In the event of an appropriate degree of matching, the direction of the known reference frame can be determined, and thus the attitude of the spacecraft. Presently, second-generation star trackers are being employed. A major advantage of these new star trackers over past systems is that no initial attitude from another source is required.

Star trackers are required to be fast, very accurate, light in weight, have low power consumption, low cost, low complexity, and be highly robust. Accuracy mainly depends on the Field Of View (FOV). The FOV size should be small for a simplified design of the camera lens, a reduction in weight, and optical distortions. The number of stars in the FOV should be large to ensure a greater number of stars for comparison. Typically, these two competing requirements are at odds with one another. The number of stars in the star catalog should be as large as needed, but

Received 15 August 2005; revision received 24 February 2006; accepted for publication 7 August 2006.
* Email: willbria@isu.edu

often, the size of the star catalog is dictated by on board storage and computational capabilities. These competing requirements and the desire for higher accuracy form the motivation for the research presented in this paper.

Recent advances in star tracker processing can be summarized as follows. Accardo[2] presents an approach for three-dimensional angular velocity determination using a star sensor in high-rate rotational modes by estimating the instantaneous velocity vector and the star position vector. These vectors are obtained by extracting the end points for each time-trace stripe in the FOV. Jørgensen et. al,[3,4] determined the attitude and attitude dynamics of Teamsat as well as conducted experiments for the radiation impacts on star tracker performance and vision systems in space using the Autonomous Vision System (AVS). The objectives were autonomous star identification, attitude determination and identification, and tracking of non-stellar objects. The AVS consisted of a CCD-based camera Head Unit (CHU) and a Data Processing Unit (DPU) including a radiation tolerant microcomputer, a star catalog, a search engine and a support structure. Gipsman et. al,[5] described the Coupled Sun Star Tracker (CSST) and the Accelerometer Vector Block (AVB) which constitute the navigator system for deep space missions. A second-generation solid-state star tracker, the Advanced Stellar Compass (ASC), which consists of a CCD camera and its integral image processing electronics, operates by matching the star images acquired by the camera with its internal star catalogs. This is accomplished by performing a spherical least-squares method between the image and the star catalog.[6]

Birnbaum[7] presents the development of star field trackers for star field recognition, resulting in three solutions: ASTROS star trackers (AST), Stellar reference unit, and ORSTED Advanced Stellar Compass. Liebe[1,8] portrays the traditional attitude determination systems, the second-generation star trackers, design of star trackers and all of the parameters that affect the performance of the star trackers. He also discusses the pattern recognition of star constellations for spacecraft applications and describes star catalogue, database and construction of these as well as the uncertainty in the database. Portelli et. al[9] presents the attitude determination using one or more CCD cameras. In addition, they describe the hardware and software components used to implement the system in the flight experiment that aims at testing the flight software and hardware in space.

McClintock et. al[10] proposed a Genetic Algorithm for star pattern recognition where the stellar catalogue provides the position, magnitude and color for all stars, which are recorded in a vector format. It was concluded that GAs arrive at or near optimal solutions within a reasonable amount of time. The GA implementation used in the present work distinguishes itself by including a "focusing" algorithm, which let's the best performing solution "spiral" to the optimum solution and allows for a predetermination of the accuracy achieved. Additionally, this algorithm is able to determine the angular displacement (or roll rotation) with respect to the celestial poles.

An attitude measurement sensor is typically required to operate in three different modes: (1) "lost in space", (2) maintain a predetermined attitude, and (3) track (or rotate) from a current to a new attitude. This paper focuses on the lost in space mode in which it is desired to determine from celestial observations the attitude (or in other terms, where the spacecraft is pointing). This paper presents the application of a unique Genetic Algorithm approach to the "Lost in Space" attitude determination problem using a star tracker sensor.

II. Genetic Algorithms

The "Lost in Space" star tracker problem can be considered an optimization problem; an imaged pattern is matched to a star catalog with the highest precision in as short as time possible. Optimization algorithms traditionally involve the computation of gradients and the application of the Weierstrass Theorem to determine the existence of a global minimum. If constraints are involved, Lagrangian multipliers are used along with the Kuhn-Tucker Theorem. Nonetheless, finding the global optimum point is not guaranteed. A different approach to the optimization problem, called Genetic Algorithms,[11] has become more and more popular in recent years. This algorithm does not involve any derivatives and is basically a numerical approach to the problem. Genetic Algorithms are evolutionary algorithms that simulate Darwin's survival of the fittest principle. These algorithms involve some amount of randomness in their procession through each step, which in turn ensures that with sufficient number of iterations (known as generations) the global optimum point will be found. In addition to the ability to find the global optimum point, a set of candidate solutions are available. The general outline for such an algorithm is shown in Figure 1.

The algorithm starts first with the generation of a randomly selected initial population of candidate solutions. This can be done with continuous numbers or in a binary format. Figure 1 reflects the binary representation, which is easier to visualize. The continuous number approach is very similar to the binary approach. The encoding of the parameters into binary format is a simple conversion from a floating-point format to binary numbers or gray

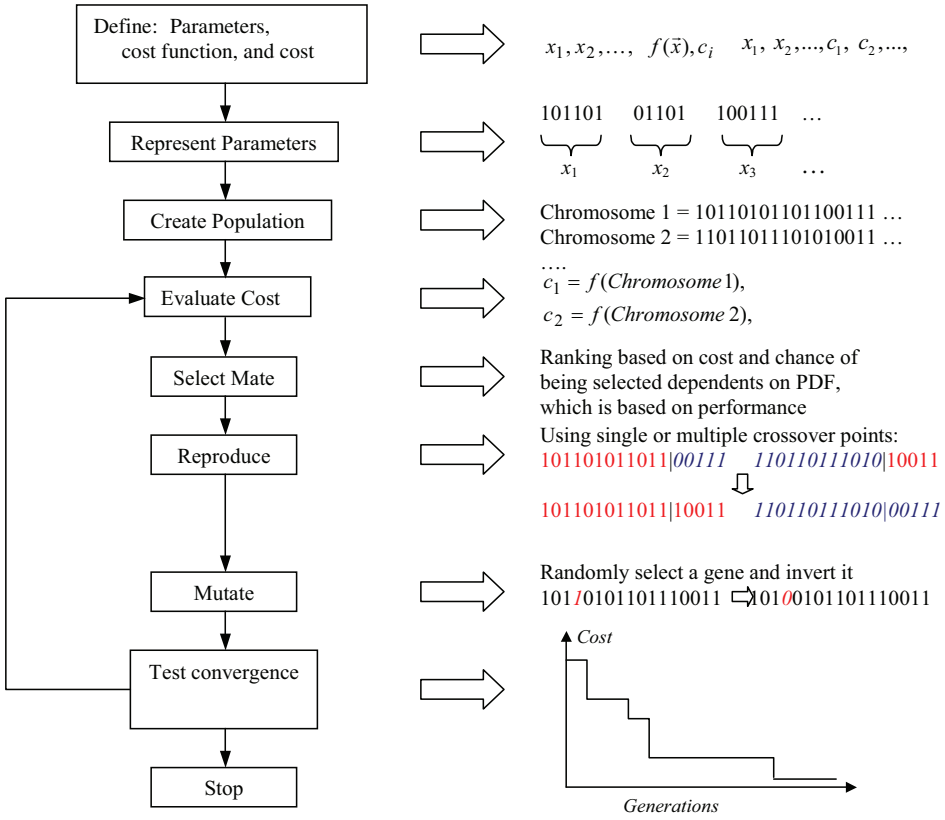

Fig. 1 Outline of a Genetic Algorithm using the binary format.

code numbers. Each parameter represents one gene and the set of parameters to describe the problem constitutes one chromosome. The generated chromosomes are evaluated based on a cost or objective function (this function is also often referred to as the fitness function) and ranked in terms of its fitness. The evaluation of each chromosome requires a translation into real numbers for each gene so that it can be computed with the given objective function. A subset of the next generation of candidate solutions is selected based on their performance with the objective function. A mating process generates the remaining sets of the new generation, where the best performing candidate solutions comprise the subset of the parents. The selection of the parents is done randomly based on the probability density function (pdf), which can be formulated based on the chromosome's performance. In particular, the pdf for the selection scheme used in this work is called the weighted random pairing algorithm (also referred to as the weighted cost selection). This algorithm assigns a probability to the chromosomes in the mating pool according to their cost function. A chromosome with the lowest cost function value has the greatest probability for mating. The mating process involves a low number of so called crossover points, where the chromosome of each parent is divided and the resulting parts are recombined with other parts of the other parent chromosome. For example, for a single crossover point the parents will generate two offspring, for two crossover points, the parents will generate three offspring, etc. In addition to the mating process, a mutation rate is also imbedded in the generation of the new population. For binary representation, the mutation is given by changing the binary bits for an arbitrary small percentage of the entire collection. The mutation enables the search for the optimum solution to overcome local minimums and 'jump' over constraint boundaries in the search space to locate the global minimum/optimum. This process of selection, mating, and mutation is repeated a number of times until the best performing candidate solution converges to some stationary value. Besides the capability of overcoming local minima, additional advantages of genetic algorithms are that they result in a set of candidate solutions, which can be used subsequently with the proposed spiraling algorithm.

III. Application of Genetic Algorithms to Star Pattern Recognition

A star sensor initiates its attitude determination routine by taking an image of a star pattern, bounded by the FOV and centered along the bore-sight. It is assumed that the FOV size is known as well as the positioning of the imaging system's bore-sight with respect to the axis of the spacecraft. Since the distance from the observer to the stars is so large, it appears as if the three-dimensional location of the stars is projected onto a two-dimensional surface, known as the celestial sphere. As such, the geometric relationships between the stars can be treated as if they are all on the same plane. Unfolding the celestial sphere results in a flat surface. The north celestial pole is aligned with the north rotational axis of the earth on such maps.

This realization of the celestial sphere as a rectangular surface presents some challenges for patterns closer to the edges of the realized map. This paper will use an accurate star map with 1000 stars and a randomly generated star map also containing 1000 stars. However, to aid the development of the algorithm and understanding the applied concepts, the distortions are assumed negligible for the randomly generated star map simulations.

The GA randomly selects a population of candidate coordinates from the star catalog. Within a distance equal to the diameter of the FOV, a star pattern is observed around the candidate coordinate (called the candidate FOV). In solving the attitude determination problem, the computed parameters of the candidate FOV and the image FOV are compared. The computed parameters used for this effort are distances to the stars ($\boldsymbol{R}$) within the FOV and the angle of rotation ($\boldsymbol{\theta}$) from a reference to $\boldsymbol{R}$. The distance to each star in the FOV is referenced from the center of the FOV (bore-sight for the imaged FOV and the candidate coordinates for the candidate FOV). The angle is referenced from the x-axis (x_i in Figure 2, also refer to Figure 5) and measured counter-clockwise to each $\boldsymbol{R}$ vector. The x-axis is either known with respect to the spacecraft's coordinate system (imaged FOV) or a horizontal line on the star catalog's celestial sphere (candidate FOV), perpendicular to celestial north. The magnitude of the $\boldsymbol{R}$ vectors for all stars in the FOV is combined into a distance vector ($\boldsymbol{D}$). The magnitude values of $\boldsymbol{R}$ are numbered sequentially, starting with the star closest to the center (smallest $|R_k|$), proceeding to the next closest, and so forth. The distance vector for the FOV imaged stars is given by

$$\boldsymbol{D_a} = [\boldsymbol{R}_1, \boldsymbol{R}_2, \ldots, \boldsymbol{R_n}] \tag{1}$$

where n is the number of stars visible in the FOV whose parameters are used in the GA routine. The subscript "a" refers to the actual (or imaged FOV) values. Angles are numbered according to the sequence above for the magnitude values of $\boldsymbol{R}$. For example, the closest star is numbered R_1 with a corresponding angle of θ_1. The θ values

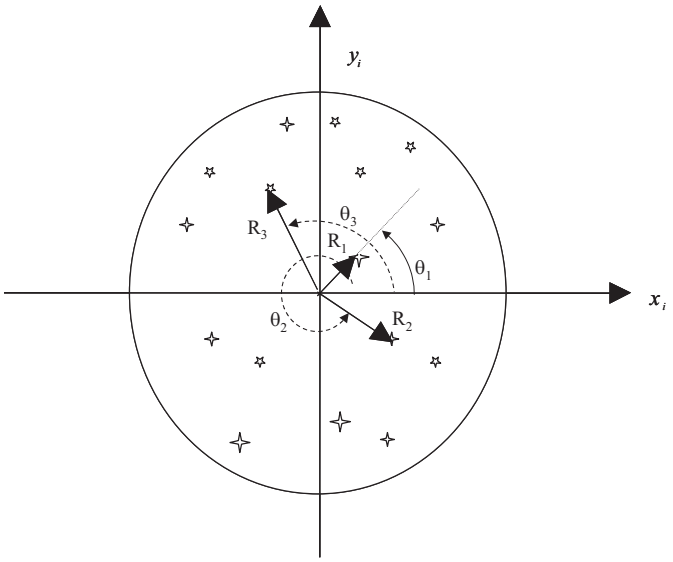

Fig. 2 Schematic showing the method for calculating the distance R and angle θ.

are combined, in order of their numbering, into an angle vector ($\boldsymbol{\theta}_a$), which can be given as

$$\boldsymbol{\theta_a} = [\boldsymbol{\theta}_1, \boldsymbol{\theta}_2, \ldots, \boldsymbol{\theta}_n] \tag{2}$$

Each chromosome generated with the GA corresponds to a candidate (x, y) location of the imager's bore-sight on the star map (x_i, y_i coordinate system in Figure 3, for the i^{th} chromosome). Based on the method described previously, a distance vector and angle vector ($\boldsymbol{D}_i$ and $\boldsymbol{\theta}_i$, respectively) is computed for each chromosome. Here, the subscript "i" refers to the i^{th} candidate FOV. A cost function (C_i) for the i^{th} chromosome is defined as the sum of the differences of R_k ($k = 1, 2, \ldots,$ n) between the actual distance vector and the chromosome's distance vector:

$$C_i = \sum_{k=1}^{n} |\mathbf{D}_a[R_k] - \mathbf{D}_i[R_k]| \tag{3}$$

The top chromosome is defined as the chromosome with the minimum cost function (lowest value of C_i) for a given generation. Once the top chromosome's cost is less than a predetermined convergence value (δ), the routine is completed and the program moves on to the next GA routine.

The star pattern recognition algorithm includes a proposed Spiral Genetic Algorithm (SGA). The SGA results in a reduction of the search area that is proportional to the minimal cost (δ) of the previous GA. The next-level GA routine bounds its search, centered around the top chromosome from the previous GA routine, extending out some value Δ on all sides. The limiting value, Δ, is determined from the size of the original FOV as well as the previous GA's target minimal cost. A new minimal cost provides a convergence criterion for the new GA routine. This process continues (spirals) until a solution is found that approximates the observed location with an error that approaches zero (see Figure 4).

Once a candidate attitude is found, the angle of rotation (ϕ) of the spacecraft with respect to the star map can be computed using another GA routine (see Figure 5). If a candidate position ($\boldsymbol{D}_i$) matches that of the imaged FOV along the bore-sight ($\boldsymbol{D_a}$), then there is a distinct constant angular value, when added or subtracted from the FOV-imaged angles, which produces a perfect match to a position on the star map. In the case no distinct single rotation angle can be determined, then the process starts over with the distance GA. The equation of the cost function for the angle of rotation (C_i') is given as follows

$$C_i' = \sum_{k=1}^{n} |\boldsymbol{\theta}_a[\theta_k] - \boldsymbol{\theta}_i[\theta_k]| \tag{4}$$

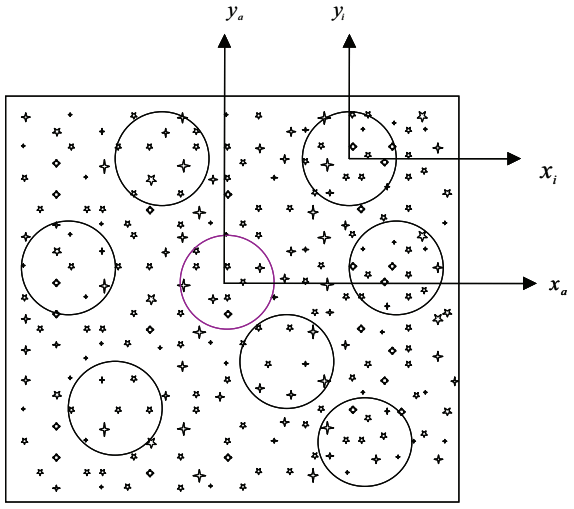

Fig. 3 Star map with chromosomes (candidate x_i, y_i locations) for the GA approach.

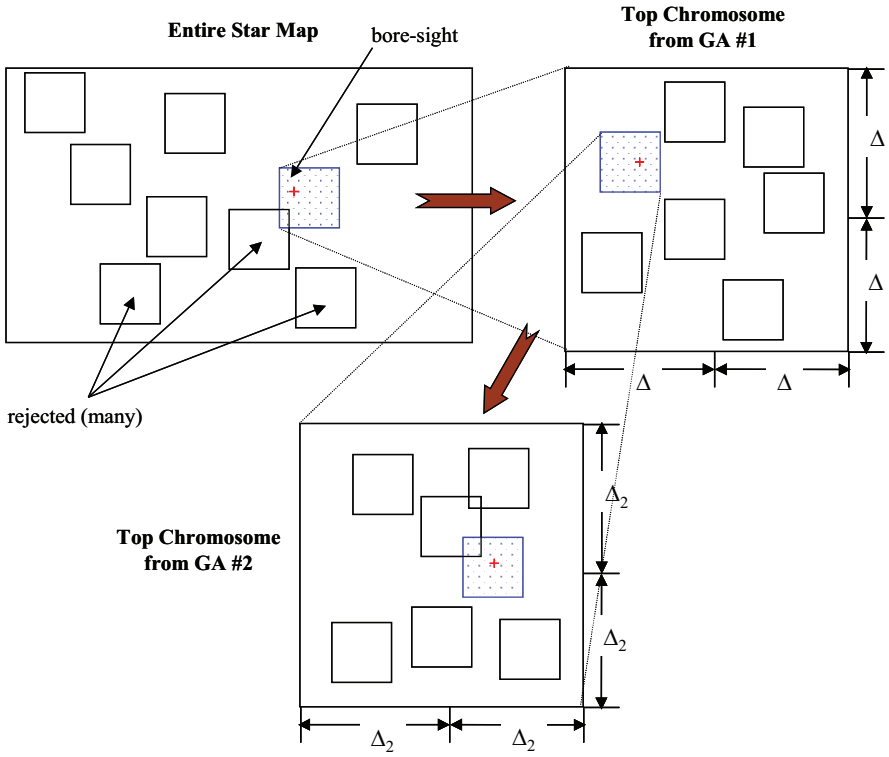

Fig. 4 Concept picture of the Spiral Genetic Algorithm approach. Note, square FOV's are used only to simplify the concept.

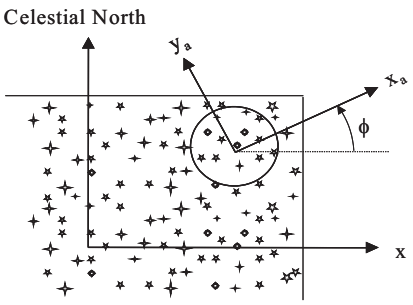

Fig. 5 Picture showing the rotation angle ϕ with respect to the celestial sphere coordinates.

IV. Simulation Setup

Simulations are carried out using the two GA's (to form a SGA) for finding the attitude using distance and one GA for calculating the angle of rotation.

The dimensions for the random star map are 300 units by 300 units (-150 to $+150$). It is assumed that the 300-unit wide star map represents a full 360° view. A circular FOV with a radius of 25 units is used. The number of stars (m) within the FOV for these particular simulation is kept between 15 and 20. If the FOV has fewer stars, then zeros are added to the beginning of the distance vector for a total of m stars (actual plus added). If the FOV has more stars, then only the m closest stars to the center are included.

The GA used for this simulation is a continuous number GA – as outlined earlier. In particular, the mating algorithm simulates the binary method, where a randomly generated crossover point is selected. Unlike for binary GAs, the crossover point for both mating charomosomes is not only used for the determination of the gene length of the gene swapping, but also to generate a new gene, that is placed at the crossover location in the new chromosome. The new gene is a linear function of the two genes located at the cross over point in the parent chromosomes. This new gene can be given as

$$gene_{new_{1,2}} = Parent_{Mother_\alpha} \pm \beta(Parent_{Mother_\alpha} - Parent_{Dad_\alpha}) \tag{5}$$

where α is the crossover point, β is a random number uniformly distributed between 0 and 1, and $\text{Parent}_{\text{Mother}}$ or $\text{Parent}_{\text{Dad}}$ are the mating chromosomes.

For the simulations using the randomly generated star map, a total of 300 initial attitudes for candidate FOVs are selected randomly, of which 150 are retained as steady-state population for each generation. The influence of these parameters is not investigated with this paper; these parameters are selected at random based upon previous experience. Of the 150 candidate FOVs, 80 are selected based on their performance measured by the cost function to survive into the new generation. 80 new FOVs are then generated using the pairing, mating, and mutation algorithm described previously and the best-performing 150 FOVs are retained for the steady state population. The mutation rate is set at 6%. None of these parameters were optimized, which could potentially increase the efficiency of the proposed algorithm. If the cost function does not converge to the expected value, a new set of chromosomes is taken and the algorithm is run from the beginning with the new chromosomes.

After the cost converges to a value less than or equal to the cost required for convergence of the first GA, the second GA that has a total of 100 initial locations of candidate FOVs refines the determined FOV location. The 100 locations are selected randomly in the region around the point where the first GA converged with some error Δ around the point of convergence. From these 100 initial locations, 50 are retained as steady state population for each generation, of which 30 are selected based on their performance given by the associated cost. The mutation rate for this stage is again kept at 6%.

To find the angle of rotation, a total of 120 initial angles (degrees) are selected randomly, of which 60 are retained and 30 are selected based on their performance, the mutation rate being the same. Again, the influence of these parameters is not investigated with this paper and these parameters are selected at random based upon previous experience

Using the same parameters and algorithms, a real star map generated from an accurate star catalog[†] is used in the second set of simulations. A real star map includes the uneven distribution of stars and thus different sensitivities within the search field, as well as expressing the position values in terms of Right Ascension (RA) and Declination (DEC). The implementation of the real star map presents three main challenges. These are i) inability of the algorithm to recognize map wrapping at the map edges; ii) that two positions on a sphere have two distinct distances apart; and iii) that the RAs converge to a conical shape at the polar regions. To reduce the distortions and minimize the sensitivities, we propose a 3-map representation of the star catalog combined with a simulated dynamic cylindrical rolling of the spherical star map. This simulated rolling perceives the spherical map realization as a cylinder instead of a flat rectangular surface. This combination thus recognizes the existence of two distinct distances between 2 positions on a sphere and selects the shortest distance due to the fact that a camera observes the shortest distance between celestial objects. The 3-map representation seeks to significantly reduce the convergence effect of the RAs at the polar regions of the celestial sphere. The maps are overlapping with each other to provide additional dynamism. These are realized through the algorithm's cost assignment routine.

The next two sections summarize the simulation results for the two star catalog implementations, the randomly generated star catalog and the actual star catalog, which contains 1000 stars selected based on brightness.

[†] CDS (Centre de Donnèes astronomiques de Strasbourg), VizieR Catalogue Service website http://cdsweb.u-strasbg.fr/viz-bin/VizieR-3 on March 2004.

All simulation results presented are based on 21 sets of simulations for 51 randomly selected FOV locations for both star map implementations.

V. Simulation Results for Randomly Generated Star Map

Multiple simulations using the GA approach are conducted in order to statistically describe the potential accuracy of the proposed algorithm (proof of concept). Results were recorded of simulation runs of the standardized map case that took about 600 generations or less for convergence to the minimum cost. The convergence was determined when the cost of the top chromosome is less than 0.001882.

The actual (imaged) location of the bore-sight was selected as the origin of the star map ($x = 0, y = 0$). A deviation of about 0.0012% in the x-coordinate and 0.000062% in the y-coordinate locations ($x_{\text{mean}} = -0.0018544$ with a standard deviation of $x_{\text{std}} = 0.0020563$ and $y_{\text{mean}} = -0.00009245$ with a standard deviation of $y_{\text{std}} = 0.000657$ units) is obeserved.

As an example, consider the results of one such simulation. The location of the FOV's bore-sight is $x = 0$, $y = 0$ with an angle of rotation of 60° (1.0472 radians). The algorithm uses 20 stars located within the FOV.

Step 1: The first GA requires a minimum cost of less than 3.0 using the distance values (see Figure 6). The top chromosome of the first GA is $x = -0.0363$ and $y = 0.2010$. The resulting cost function value is 2.1825.

Step 2: The second GA requires a minimum cost of less than 1.0 using the given distance values (see Figure 7). The search area for potential candidate locations (chromosomes) is decreased to a square whose center coincides with the location of the top chromosome from the previous GA ($x = -0.0363$ and $y = 0.2010$). The size of the search box is equal to $\Delta = \pm 2.40075$ units; this corresponds to a high-end x value of 2.36445 units and a low-end x value of -2.43705 units. For the y axis, the high-end value is 2.60175 units and the low-end value is -2.19975 units. From this second GA, a top chromosome of $x = -0.0059$ and $y = -0.0031$ is found, with a cost function value of 0.0065.

Step 3: Since convergence to the x, y value was achieved, another GA to find the rotational angle, ϕ, is used. The range of chromosomes considered varies from 0° to 360°s. The top chromosome for this GA is 60.0001°(corresponding to 1.0472 radians), which is approximately the same as the actual rotation angle. The minimum cost function value for this GA is 0.0003712 (see Figure 8).

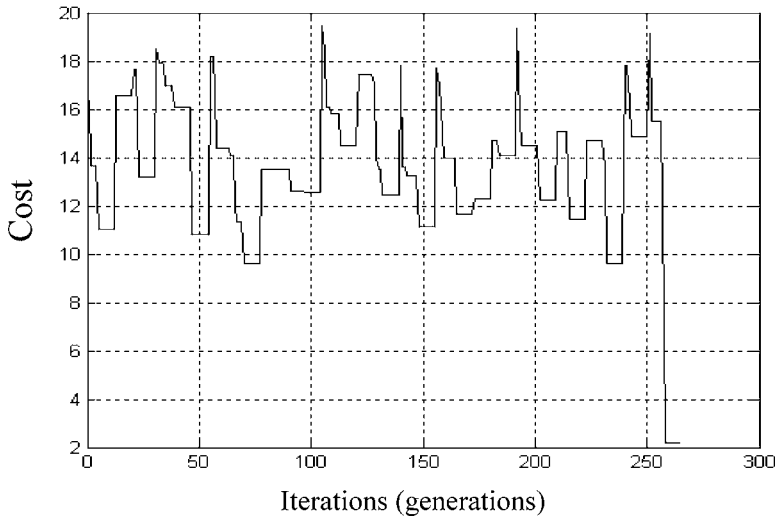

Fig. 6 Plot of cost function versus number of iterations for the first GA.

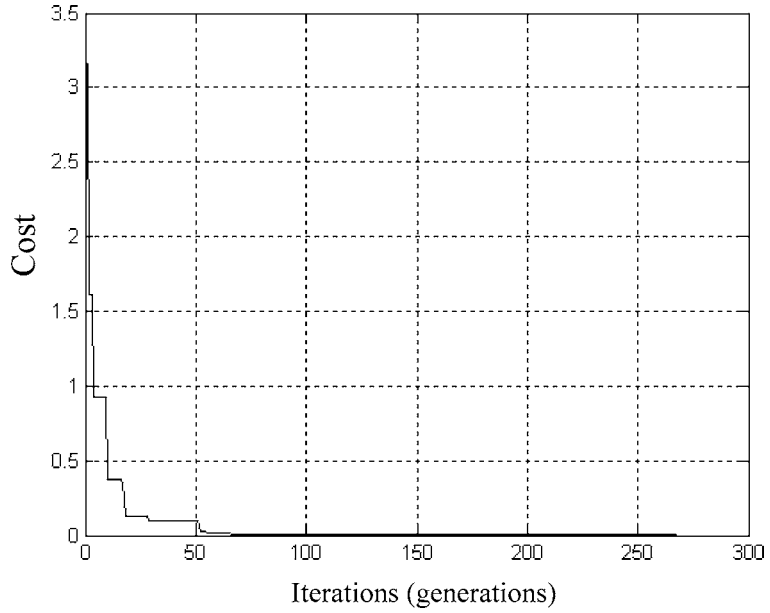

Fig. 7 Plot of cost function versus number of iterations for the second GA.

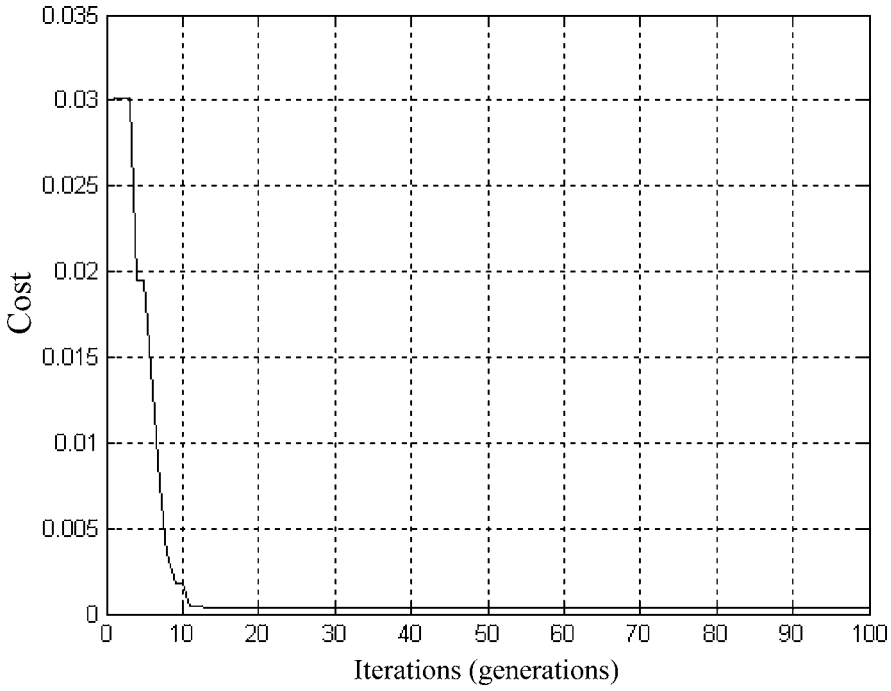

Fig. 8 Plot of cost function versus number of iterations for the rotation angle GA.

VI. Simulation Results Using an Actual Star Catalog

The results obtained for the real star catalog case is presented in Table 1. The results exclude a rotational angle calculation since it is determined to be independent of map realization. Note that a transition takes place in which values are now represented in degrees compared to the x-y values in Cartesian coordinates; the change to degrees

Table 1 Real star catalog performance characteristics with origin FOV.

	Angular value [degrees]
x-coordinate (Yaw)	−0.0182
y-coordinate (Pitch)	0.0099
Recognition error	0.0208

allows an easier transition with the actual star map data (RA and DEC) as well as easier comparison between yaw/pitch angle resolution of existing sensor systems. In place of coordinates given by (x, y), they will now be given by (RA, DEC) with units of degrees. Additionally, variations in the "x" direction (now RA) will be correlated with the yaw direction and variations in the "y" direction (now DEC) will be correlated with pitch.

For a typical simulation to estimate an FOV with bore sight at the origin (0°, 0°) using the same parameters as those for the standardized (randomly generated) map, the results for the real star catalog correspond to those of the standardized (random) map. The observed best-candidate FOV bore sight is at (−0.0182°, 0.0099°), which also gives a measure of the deviations in the coordinates. The recognition error, measured in terms of the distance norm between the desired and observed bore sights is determined to be 0.0208°. The minimum cost achieved is 0.0174°.

Table 2 presents the mean value of the results for arbitrary FOV locations identified by arbitrary bore-sights and fixed FOV size using the real star catalog. A typical cost profile of the best performing chromosome (lowest cost) of each generation for the spiral GA is presented in Figure 9.

From Table 2, the average deviations for the random FOV observations in the coordinates are 0.149°(yaw) and 0.005° (pitch) with a standard deviation of 0.1013° and 0.0008°, respectively. In respect of the recognition error

Table 2 Real star catalog performance characteristics with random FOVs.

	Mean of deviations	Standard deviation of means
x-coordinate (Yaw)	0.1489°	0.1013°
y-coordinate (Pitch)	0.0051°	0.0008°
Recognition error	0.0157°	0.0376°

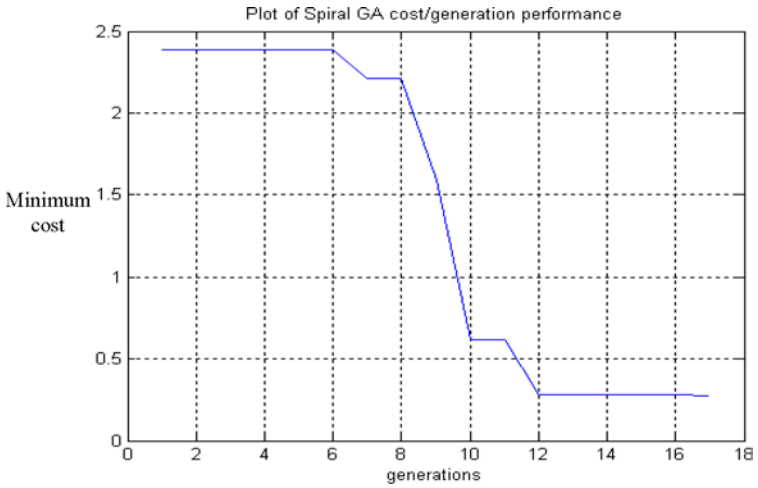

Fig. 9 Spiral GA cost function generation history.

(distance norm), which is a measure of the pointing accuracy for the spacecraft, the obtained average is 0.016° with a standard deviation of 0.038°.

VII. Discussion of Simulation Results

For the simulations of the simulated map, the accuracy levels obtained for both the x and y directions are on average 0.0071° and 0.0037° values for Cartesian coordinates with (x, y) units were converted to angles (degrees) by assuming that the range of x & y equaled 360° rotation. Using the mean values of all simulations for the simulated map and the real star catalog, the mean overall accuracy level of the two GA routines (the pointing accuracy) is 0.0157°. As a comparison, the EMS Technologies CALTRAC^{TM} Star Tracker has a noise angle of $\pm$0.005° in the pitch/yaw direction [12]. The results obtained for the real star catalog is thus within an acceptable range. Given that the parameters used in the algorithms are not optimized in any way, there may be room for improvement.

To increase the accuracy of the SGA technique, additional GA's could be used with successive decreasing search areas and cost functions.

The application of the proposed GA based algorithms for star pattern recognition can still be improved by optimizing the parameters so that the position is more accurately known and achieved at a faster time. The number of stars in the star catalog is directly proportional to the speed of convergence of the algorithms whilst, the number of stars in the FOV is proportional to the cost achieved. As the number of stars in FOV increases, the cost function value increases. With a greater number of stars there is a better possibility of finding the exact, distinct position of the image. For this work, the x and y coordinates used are the right ascension and declination values of a typical stellar catalog.

Generally, attitude determination should not consume a lot of time due to the rapid changes in attitude of space objects. Therefore, computational time should be at a minimum. The simulations used in this work originate from a single processor computer running all code in Matlab© (usually slower than running pure compiled code). One potential method to increase computational speeds of the algorithm proposed is to involve parallel processors. Currently, the single processor calculates the parameters of each chromosome (candidate FOV) in a sequential form, and then sequentially compares them to the actual (imaged) parameters. Multiple parallel processors will allow each individual processor to compute the candidate's parameters and cost function. A single processor can then sort the cost values to determine the top chromosome for the iteration. The advantage of the parallel processing system would be simultaneous computation of redundant multiple calculations. Disadvantages could include an increase in hardware complexity, cost, and power consumption.

Another option is to use the brightness (or magnitude rating) of a star as a pre-computation filter. In choosing GA-selected candidate positions, a comparison is first made between the magnitude of the star closest to the bore-sight and the star closest to the GA-selected position. If the candidate's magnitude is not within a given value of the star nearest the bore-sight, then there is no need to compute the distance vector, $\mathbf{D}_i$, and hence a cost function. Distance vectors and cost functions would be computed only when the candidate star's magnitude is within the required magnitude of the bore-sight star.

VIII. Conclusions

The efforts presented in this paper successfully demonstrate the ability of Spiraling Genetic Algorithms to perform the pattern-matching computations associated with the "lost in space" mode of a star sensor, for a real star map. Simulation results indicate a recognition error of 0.0157° (equivalent to yaw/pitch directions), which is within the current accuracies of commercial systems. To further increase the accuracy of the Genetic Algorithm approach, successive (spiraling) routines may be added with decreasing search pattern size and convergence criteria (cost). Even though no statistics were computed for the roll rates, the Genetic Algorithm approach presented in this work demonstrated the ability to successfully determine the "roll" rotation angle of the imaged pattern with respect to the celestial sphere's poles.

Future efforts will concentrate on optimizing the Genetic Algorithm control parameters and genetic operators such as the selection operator, the pairing and mating scheme, the mutation operation, as well as population size, FOV size, etc. towards decreasing the required computational time and required power.

Acknowledgements

This work was partially funded by an ISU infrastructure grant. The support is greatly appreciated.

References

[1]Liebe, C. C., "Pattern Recognition of Star Constellations for Spacecraft Applications", *IEEE Aerospace and Electronic Systems Magazine*, Vol. 8, No. 1, Jan. 1993, pp. 31–39.

[2]Accardo, D., "A Procedure for Three-Dimensional Angular Velocity Determination using a Star Sensor in High-Rate Rotation Modes", *Acta Astronautica*, Vol. 48, No. 5–12, 2001, pp. 311–320.

[3]Jørgensen, J. L. *et al.*, "Radiation Impacts on Star-Tracker Performance and Vision Systems in Space", *Acta Astronautica*, Vol. 46, Nos. 2–6, 2000, pp. 415–422.

[4]Jørgensen, J. L. *et al.*, "The Determination of the Attitude and Attitude Dynamics of Teamsat", *Acta Astronautica*, Vol. 46, Nos. 2–6, 2000, pp. 423–432.

[5]Gipsman, A. *et al.*, "Autonomous Navigation and Guidance System for Low Trust Driven Deep Space Missions", *Acta Astronautica*, Vol. 44, Nos. 7–12, 1999, pp. 353–364.

[6]Eisenman, A., "Operation and Performance of a Second Generation, Solid State, Star Tracker, the ASC", *Acta Astronautica*, Vol. 39, Nos. 9–12, 1996, pp. 697–705.

[7]Birnbaum, M., "Spacecraft Attitude Control using Star Field Trackers", *Acta Astronautica*, Vol. 39, Nos. 9–12, 1996, pp. 763–773.

[8]Liebe, C. C., "Star Trackers for Attitude Determination", *IEEE Aerospace and Electronic Systems Magazine*, Vol. 10, No. 6, June 1995, pp. 10–16.

[9]Portelli, C., *et al.*, "A Flight Demonstration of the Stellar Autonomous Attitude Determination System on SAC-C", *Proceedings 4*th *ESA International Conference on Spacecraft Guidance, Navigation and Control Systems*, ESTEC, Noordwijk, The Netherlands, 18–21 October 1999 (ESA SP-425, February 2000).

[10]McClintock, S. *et al.*, "The Application of Genetic Algorithms to Star Pattern Recognition," Methodologies for the Conception, Design, and Application of Intelligent systems, *Proceedings of IIZUKA'96*, pp. 541–544.

[11]Haupt, R. L., and Haupt, S. E., *Practical Genetic Algorithms*, John Wiley and Sons, Inc., New York, 1998.

[12]EMS Technologies, Inc., "EMS Space & Technology – Commercial Space Products – Optical: CALTRAC™ Star Tracker," http://www.emsstg.com/science/optical.asp, accessed 10 June 2003.

J.A. Mulder
Associate Editor